Impact of Microextrusion and Addition of Graphite Nanoplatelets on Bulk and Surface Mechanical Properties of UHMWPE

Jose-Alejandro Delgado-Rangel,[1] Frédéric Addiego,[1] Fatima Eddoumy,[1] Saïd Ahzi,[2] Stanislav Patlazhan,[3] Valérie Toniazzo,[1] David Ruch[1]

[1]*Advanced Materials and Structures Department, Public Research Centre Henri Tudor, 66 Rue de Luxembourg, L-4221 Esch-sur-Alzette, Luxembourg*
[2]*Institut de Mécanique des Fluides et des Solides, Université de Strasbourg, 2 Rue Boussingault, F-67000 Strasbourg, France*
[3]*Semenov Institute of Chemical Physics, Russian Academy of Science, Kosygina Street 4, 117977 Moscow, Russian Federation*

Received 30 November 2011; accepted 30 November 2011
DOI 10.1002/app.36594
Published online in Wiley Online Library (wileyonlinelibrary.com).

ABSTRACT: A new processing route for producing ultra-high molecular weight polyethylene (UHMWPE) nanocomposite combining swelling in toluene, microextrusion, and compression-molding was developed. Using this novel method, extruded neat UHMWPE (e-PE), and extruded UHMWPE blended with 0.5 wt % of graphite nanoplatelets (e-PE/g) were processed. UHMWPE was also processed by compression-molding (PE) as reference material. Bulk mechanical behavior of the materials was evaluated by tensile, bending and impact tests, while surface mechanical behavior was assessed by scratch and sliding wear experiments. We found that e-PE/g has a brittle tensile behavior in comparison with the two other grades. Bending and impact toughness increase in this order: PE $\approx$ e-PE/g $<$ e-PE. Scratch behavior of the materials is quite similar, e-PE has however the lowest friction coefficient, and hence, exhibits antifriction properties. The cumulative sliding energy increases in this order: e-PE $\approx$ PE $<$ e-PE/g, indicating that e-PE/g may have a lower wear resistance as compared to the two other materials. The combination of extrusion with compression-molding caused the formation of well-consolidated meso-domains containing oriented chains. Such a new morphology is at the origin of the high tensile strength, high fracture toughness, and antifriction properties of e-PE that appears like a promising material for medical or machine construction applications. The addition of graphite nanoplatelets induces a poor consolidation that resulted from the segregation of the fillers between powder grains of UHMWPE. This explains the brittle tensile behavior and the high cumulative sliding energy of the UHMWPE nanocomposite. © 2012 Wiley Periodicals, Inc. J Appl Polym Sci 000: 000–000, 2012

Key words: biomaterials; extrusion; nanocomposites; mechanical properties; UHMWPE

INTRODUCTION

Ultra-high molecular weight polyethylene (UHMWPE) is widely used in medical application as bearing surface in artificial joints and in machine construction as highly abrasion-resistant component. Because of its extremely long chain length and its high viscosity at the molten state, the consolidation process of this polymer is achieved by sintering. This process requires a subtle combination of temperature, pressure, and time to create a self-diffusion mechanism of polymer chains between adjacent grains.[1–3] Thus, semifinished UHMWPE components are ordinarily processed by compression-molding or ram-extrusion with well-defined conditions. To increase mechanical properties of UHMWPE, as for example elastic modulus, tensile strength and toughness, this material can be blended with micro/nanoparticles or fibers before consolidation.[4] But, to date, attempts to develop UHMWPE composites with increased mechanical properties generally failed. In the case of medical applications, it was shown at laboratory level that UHMWPE can be blended with biocompatible nanoparticles as hydroxyapatite[5] or microfibers as carbon fibers.[6] Nevertheless, it is to be noticed that the longevity of such composites is not well-established at clinical level for total hip or knee arthroplasty. The blending step of UHMWPE powder with the reinforcing agent is generally performed manually by grounding,[7] by using a ball-milling,[5,8] or using a mixer[9] prior to compression-molding. This blending can be further optimized, enhancing polymer chain mobility by swelling in toluene[10] or in paraffin oil.[5,7] However, an optimal

Correspondence to: F. Addiego (frederic.addiego@tudor.lu).
Contract grant sponsors: Fonds National de la Recherche Luxembourg.

filler distribution and dispersion within UHMWPE, as well as an optimal filler/matrix interaction, are only achieved in a limited number of studies where an effective reinforcement of UHMWPE is noted.[5]

We developed a novel processing route to blend UHMWPE with nanofiller. The selected nanofiller is graphite nanoplatelet (10 nm-thick) due (i) to its potential bio-compatibility for medical applications, since the biocompatibility of graphite fiber was proved to be satisfactory[11] and, (ii) to the irradiation crosslinking performed in the case of UHMWPE used in artificial joints may create crosslinks between the polymer chain and the graphite platelets, and hence, it may increase interactions between UHMWPE and the filler.[8] The developed processing route included a first step consisting of dispersing graphite aggregates in toluene by ultrasonication. During this step, UHMWPE powder was added to the mixture to generate a surface swelling phenomenon of UHMWPE. This swelling process may increase chain mobility in the polymer, making easier the penetration of filler within the matrix. In a second step, the mixture was homogenized by means of a microextruder equipped with conical twin-screws. The specific geometry of the screws, coupled with an elevated temperature and high screw speed, was expected to create optimal shear and extensional flows to further distribute and disperse graphite within UHMWPE, respectively. In the same time, this equipment generated a sintering of UHMWPE. The last step consisted of pelletizing the extruded rods and producing plates from extruded pellets by compression-molding.

The objective of this work was to study the impact of microextrusion and the addition of graphite nanoplatelets on bulk and surface mechanical properties of UHMWPE. To this end, three materials were produced: (i) a reference UHMWPE, only processed by compression-molding (PE), (ii) a neat extruded and compression-molded UHMWPE (e-PE), and (iii) an extruded and compression-molded blend of UHMWPE with 0.5 wt % of graphite (e-PE/g). Tensile, bending, and impact tests were performed to evaluate bulk mechanical properties of the new materials, while scratch and sliding wear tests were done to assess their surface mechanical behavior. The mechanisms responsible for the possible enhancement of mechanical properties were elucidated by scanning electron microscopy (SEM) and wide-angle X-ray scattering (WAXS) investigations.

EXPERIMENTAL

Materials

Neat UHMWPE powder was provided by Ticona (Ticona GmbH, Oberhunsen, Germany) under the reference name GUR 1050 (molecular weight 5×10^6 g/mol). Graphite particles are 10 nm-thick platelets with a diameter below 10 μm. They are produced and commercialized by Angstron Materials (Dayton, USA) with the reference N006-010-N.

Processing

The processing consisted of three steps. In the first step, graphite aggregates were dispersed in a 99.5 wt% toluene (Carl ROTH GmbH, Karlsruhe, Germany) bath at 80 °C by means of an ultrasonic tip. Once the graphite was totally dispersed (after 15 min. of ultrasonication), UHMWPE powder was added to the mixture. The ultrasonication was pursued to homogenize the mixture color and to generate the swelling of UHMWPE. The mixture color became homogeneous (black) after 30 min. of ultrasonication. We noted that longer ultrasonication time did not influence the penetration state of the graphite within polyethylene matrix induced by the swelling, and hence, we systematically used 30 min. as ultrasonication time. Subsequently, the toluene was partially eliminated. During the second step, the mixture was introduced in an Xplore 15 mL microextruder (DSM, Geleen, The Netherlands) that was used at 220°C, with a screw rotation speed of 150 rpm, with argon gas to avoid oxidation, and without recirculation of the polymer. Finally, in the third step, the extruded/sintered rods (about 3 mm in diameter) were pelletized into 5 mm-long cylinders and introduced into a specific cylindrical mold. Note that the pellets were randomly placed within the mold to avoid preferential orientation of the polymer chains within the plates. Indeed, it was previously shown that extrusion causes a preferential orientation of polymer chain along the extrusion direction, which has a significant effect on mechanical properties and particularly on crack growth propagation.[12] 5 mm-thick disks with a diameter of 110 mm were compression-molded with a Carver laboratory press (Carver Inc, Wabash, USA). The compression-molding procedure consisted of (i) heating the material at 240 °C during 30 min at a low pressure of 2.5 bars to facilitate inter-grain diffusion of UHMWPE chains, (ii) increasing the pressure up to 20 bars during 15 min at 240 °C to increase the consolidation and, (iii) cooling the material down to 23 °C at 20 bars by using a room-temperature water circulation within the press plates. Note that two materials were produced based on the above processing route: neat extruded UHMWPE (e-PE) and extruded blends of UHMWPE with 0.5 wt. % of graphite (e-PE/g). The reference material was UHMWPE only processed by compression-molding (PE).

Scanning electron microscopy

Microstructure of the materials was characterized by means of a pressure-controlled SEM FEI Quanta

FEG 200 (FEI Company Europe BV, Eindhoven, The Netherlands). The electron beam was generated at 5kV, while the images were recorded by means of the large-field detector (LFD). The chamber pressure was set to 150 Pa using water. SEM observations were performed on cryo-fractured specimens (study of initial microstructure), on scratched specimens (study of scratch grooves) and on fractured specimens (study of bending mechanisms).

Wide-angle X-ray scattering

We conducted WAXS tests using a Panalytical X'Pert Pro MPD device (Panalytical B.V., Almelo, The Netherlands). The used radiation was the Kα of cupper ($\lambda = 0.154$ nm) generated at 45 mA and 40 kV. Detection was performed by means of the 1D detector PIXcel (Panalytical B.V., Almelo, The Netherlands). WAXS provided the initial weight crystallinity of the material based that was calculated as follows. The diffractograms were deconvoluted with the software PeakFit (Systat Software, Chicago, IL) that enabled us to determine the scattering bump area (amorphous phase) and diffraction peaks area (crystalline phase) of UHMWPE. The weight index of crystallinity was then calculated as the ratio of total crystalline peaks area to the total scattering area (including total crystalline peaks area and amorphous bump area). The measurements of crystallinity were done on 5 mm-thick specimens carefully cut from the plates of PE, e-PE, and e-PE/g. We also carried out WAXS experiments to qualitatively study the orientation state of the polymer chains during the processing steps. To this end, we recorded the scattering intensity of the orthorhombic crystalline planes (110) and (200) as a function of azimuthal angle. Such an analysis was performed on the initial UHMWPE powder (powder thickness 1 mm), and on 1 mm-thick specimens carefully cut from (i) an extruded rod before compression-molding, (ii) an extruded rod after compression-molding (specimen cut from a plate of e-PE), and (iii) a plate of the reference material (PE).

Tensile tests

Nominal tensile tests were carried out by means of an Instron 8031 servo-hydraulic testing machine (Instron France, Elancourt, France) on nonstandard dog-bone shaped specimens. These specimens were machined from the compression-molded plates and have a thickness of 5 mm, an overall length of 60 mm, and a maximum width of 20 mm. The calibrated part of tensile specimen has a length of 30 mm and a minimum width of 10 mm. Note that the radius of curvature of the calibrated part is 60 mm. Tests were performed with a crosshead rate of 1 mm/min and at room temperature (25°C).

Three-point bending tests

Three-point bending tests were done with an Instron 8031 machine on $60 \times 20 \times 10$ mm^3 single edge notched (SEN-B) samples. Note that such specimens were machined from compression-molded plates, but in this case the compression-molding procedure was performed on a higher amount of powder to obtain a plate thickness of 10 mm instead of 5 mm. Notches were made with a steel blade in the middle part of the specimen with a depth of 2 mm. A span distance of 40 mm was selected. Notched-specimens were left to recover one day before the mechanical tests. Tests were performed with a crosshead rate of 1 mm/min and at room temperature (25°C). We report in this article the evolution of cumulative bending energy (J) as a function of deflection (d) calculated from the relationship $J = (\Delta d \times F)/S$, where Δd is the deflection increment, F is the load, and S is the initial ligament section.

Impact tests

Charpy impact tests were performed on the same sample geometry as that used for the three-point bending experiments. These tests were carried out at room temperature (23°C) by means of a 300 J Charpy hammer (Schenck-Trebel GmbH, Ratingen, Germany) with a span distance of 40 mm.

Scratch tests

Scratch tests were performed on a NST nanoscratch tester (CSM Instruments SA, Peseux, Switzerland) with a diamond-like-carbon conical indenter of 5 μm in radius and an angle of 90° for the cone. For each material, 3 scratches with a length of 2 mm where generated with a normal load of 300 mN and a constant speed of 17 μm/s. We measured the average coefficient of friction μ, the average penetration depth P_d, the average residual depth R_d, and the corresponding surface recovery $r = 100 \times (1–R_d/P_d)$. Penetration depths were measured by means of the nanoscratch tester during the scratching, while residual depths were measured just after the load release by a tip scanning in the scratch groove at 1 mN and 17 μm/s.

Wear sliding tests

Sliding wear tests were carried out with computer controlled tribometer (MTM department, Katholieke Universiteit Leuven, Leuven, Belgium) configured to generate reciprocating linear sliding. The experiments were done without lubricant (dry conditions) at the temperature of 23°C and the relative humidity of 50%. We used the ball-on-plate configuration (corundum balls with a diameter of 10 mm), with a

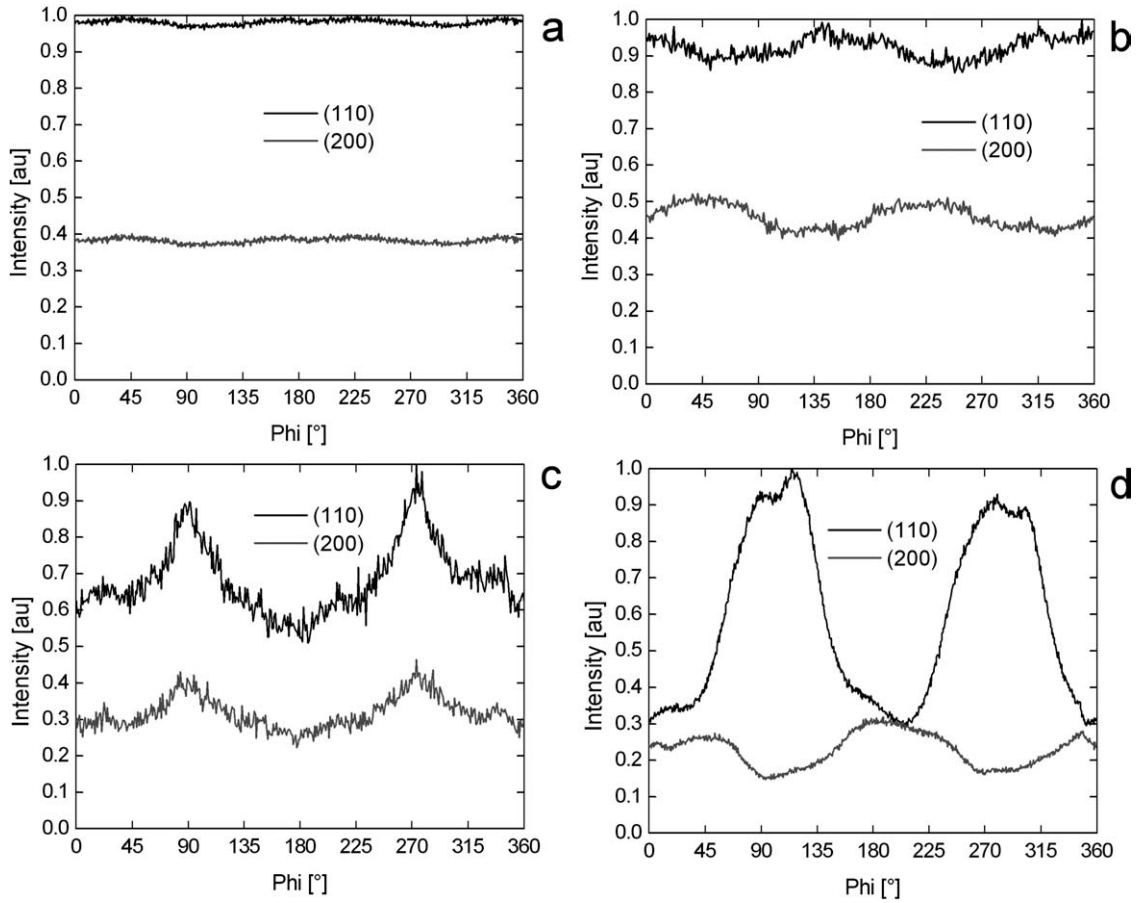

Figure 1 Azimuthal scans of the intensity scattered by the orthorhombic crystalline peaks (110) and (200) of (a) the initial UHMWPE powder, (b) compression-molded UHMWPE (PE), (c) extruded UHMWPE and (d) extruded and compression-molded UHMWPE (e-PE); for (a) and (b) the azimuthal angle 0° is selected randomly, while for (c) and (d), the azimuthal angle 0° corresponds to the extrusion direction.

normal force of 5 N that induces a calculated Hertzian contact pressure of ~36 MPa (calculations based on an elastic modulus E of 900 MPa and a Poisson's ratio ν of 0.4). Fretting sliding movements were made over 200 μm, with a frequency of 5 Hz during 50,000 cycles. These experiments and their analysis were performed according to the procedure published by Mohrbacher et al.[13] Particularly, we determined the evolution of the dissipated energy E_d (corresponding to the tangential force vs. displacement loops area) with sliding cycles. We also calculated the cumulated dissipated energy ΣE_d as a function of sliding cycles. Note that because of the low number of sliding cycles, we were not able to calculate a wear volume or wear weight loss with enough precision in this study.

RESULTS AND DISCUSSION

Physical properties

The weight index of crystallinity of the materials measured by WAXS is 50 ± 2 wt % for PE, 47 ± 2 wt % for e-PE and 43 ± 2 wt % for e-PE/g. These results demonstrate that the extrusion step performed before the compression-molding step does not significantly influence the crystallinity of UHMWPE. Nevertheless, the addition of graphite nanoplatelets slightly reduces the crystallinity of the polymer. This can be explained by a growing limiting effect of the graphite that restricts molecular movement and hinders orderly packing of molecular segments during the crystallization.[14,15]

The influence of processing step on the chain orientation state of UHMWPE is plotted in Figure 1. The initial powder, prior consolidation, is characterized by a homogeneous scattering intensity of the orthorhombic peaks (110) and (200) whatever the azimuthal angle is [Fig. 1(a)]. Once this powder submitted to hot-pressing [Fig. 1(b)], one notes a weak but significant chain orientation anisotropy, which demonstrates that compression-molding caused an orientation phenomenon of the polymer chair. When UHMWPE is extruded by our microextruder, an important orientation mechanisms occurred along the extrusion direction, as is shown by the intensity reinforcement at the azimuthal angle 90° and 270°

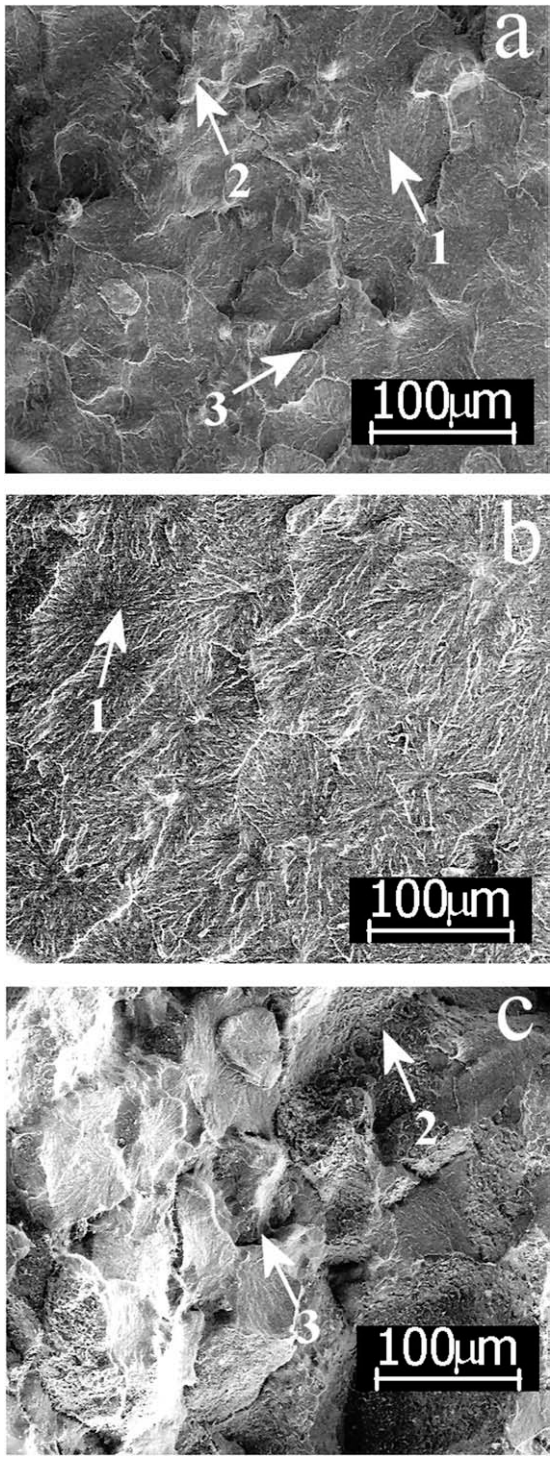

Figure 2 SEM micrographs of cryo-fractured (a) PE, (b) e-PE, and (c) e-PE/g (1: intragranular fracture, 2: intergranular fracture, and 3: consolidation defect between grains).

[Fig. 1(c)]. Such a mechanism is enhanced by a subsequent compression-molding step [Fig. 1(d)]. These results indicate that our new processing method leads to the formation of meso-domains, i.e., the former extruded pellets, containing oriented chains. The orientation level of these chains is much more marked than that observed for the reference material (PE).

Cryo-fractured morphology of PE, e-PE, and e-PE/g is shown in Figure 2. The reference material (PE) is characterized by intragranular fractures (flat area) and intergranular fractures (rough area) [Fig. 2(a)]. We also note in this material the presence of consolidation defects between adjacent grains. Regarding e-PE [Fig. 2(b)], macroscopic stresses appear to be mainly accommodated by intragranular fractures. Moreover, less consolidation defects are observed for e-PE compared to PE. SEM micrograph of the UHMWPE composite (e-PE/g) displays marked intergranular fractures revealing the presence of the graphite platelets on the fracture footprints [Fig. 2(c)]. We also note an important number of consolidation defects between adjacent grains that seems to be due to the presence of the fillers. These results prove that our new processing route leads to a good consolidation for neat UHMWPE, but to a poor consolidation for the nanocomposites that is due to a segregation of the graphite nanoplatelets at the surface of UHMWPE grains. Therefore, the combination of swelling in toluene with microextrusion is not an efficient method to homogeneously distribute graphite within UHMWPE matrix. Swelling is controlled by diffusion mechanisms, themselves driven by osmotic pressure in which solvent molecules diffuse within the polymer matrix.[5] A disengagement between polymer chains was expected to occur, which would facilitate the penetration of the filler within the polymer matrix. It is thought that this penetration mechanism was not active in our work because of the important diameter of the graphite platelets (below 10 μm). A SEM micrograph of an area containing the graphite nanoplatelets is shown in Figure 3. It can be seen that although the overall distribution of the filler with UHMWPE

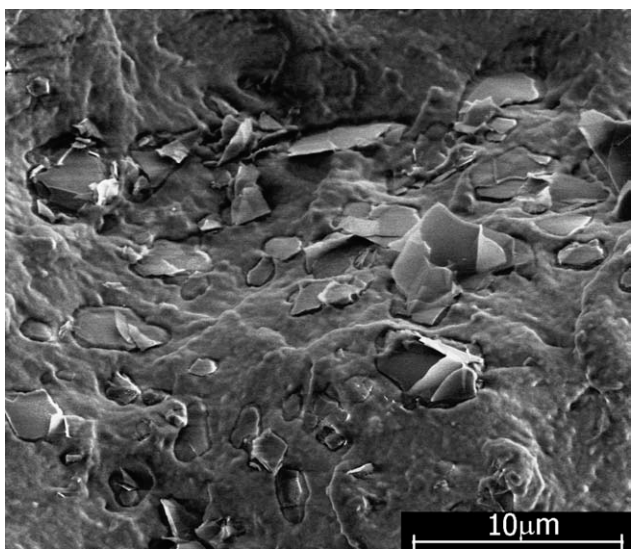

Figure 3 SEM micrographs of cryo-fractured e-PE/g showing the local distribution of graphite nanoplatelets.

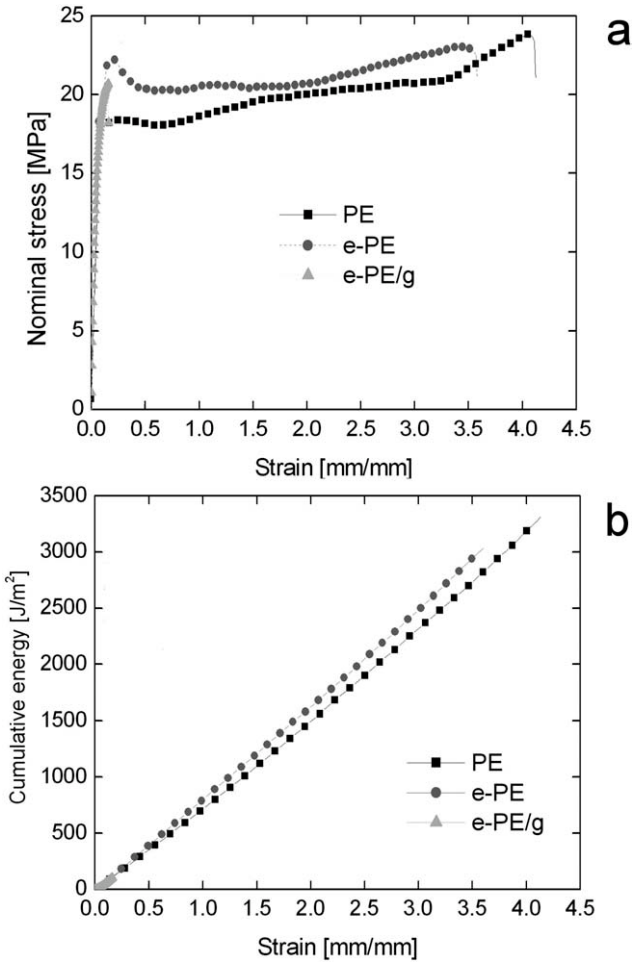

Figure 4 Tensile behavior of PE, e-PE, and e-PE/g; (a) stress–strain curves and (b) energy accumulation.

matrix is poor, the local distribution of the platelets, i.e., the dispersion, is satisfactory since little aggregation is found. This proves the efficiency of toluene to disperse graphite and/or the efficiency of the extensional flow generated by microextrusion.

Bulk mechanical behavior

Nominal tensile behavior of the materials is represented in Figure 4. We note that PE and e-PE have a ductile behavior, while e-PE/G has a brittle behavior. Indeed, this material breaks at a limited strain level (0.1) during viscoelastic deformation stage thus, it does not show viscoplasticity. The neat extruded UHMWPE (e-PE) has higher yield stress than the reference UHMWPE (PE) (22.2 vs. 18 MPa), and more generally exhibits a higher tensile strength. However, the elongation to failure of e-PE is lower than that of PE (strain at break of about 3.5 vs. 4) [Fig. 4(a)]. We also calculated the accumulated energy during the tensile test that reflects the tensile toughness [Fig. 4(b)]. e-PE/g has a cumulated energy of 100 J/m^2, while the two other materials, PE and e-PE, have a cumulated energy of 3350 and 3000 J/m^2, respectively. The brittle tensile behavior of the UHMWPE-based nanocomposite may be explained by the segregation of the filler at the grain boundaries of the matrix [Fig. 2(c)]. Such a structural heterogeneity induces a stress localization at grain boundaries, that generates first intergranular separation by the formation of defects (voids), second a coalescence of the defects, and last the failure of the specimen. The superior tensile strength of neat extruded UHMWPE as compared to the reference UHMWPE grade can be explained by its specific morphology composed of randomly oriented textured-domains, as demonstrated by WAXS measurements (Fig. 1). It is supposed that when such a morphology is submitted to tension, a stress transfer occurs from domains having a low-strength, i.e., domains whose texture is perpendicular to tensile direction, to domains having a high strength, i.e., domains whose texture is along tensile direction. The ability of e-PE to withstand stress is locally linked to a high involvement of tie molecules and entanglements in the textured-domains with chains oriented along tensile direction.[16,17] This high strength may be responsible for an important strain recovery after unloading.[18] However, it is thought that these highly-strength domains have a low-ductility since less chain extensibility is available, which may explain the lower tensile toughness of e-PE as compared to PE despite its higher strength.

The evolution of cumulative energy with deflection of PE, e-PE, and e-PE/g subjected to three-point bending tests is displayed in Figure 5. It is important to note that the bending tests conducted in this article were stopped at a deflection of 13 mm (limit of the equipment). At this value of deflection, none of the material was entirely fractured. We observe that the cumulative energy, or the fracture toughness,

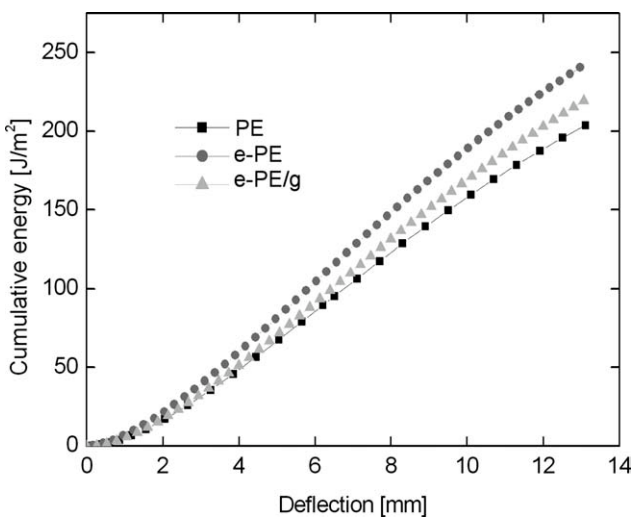

Figure 5 Flexural behavior of PE, e-PE, and e-PE/g.

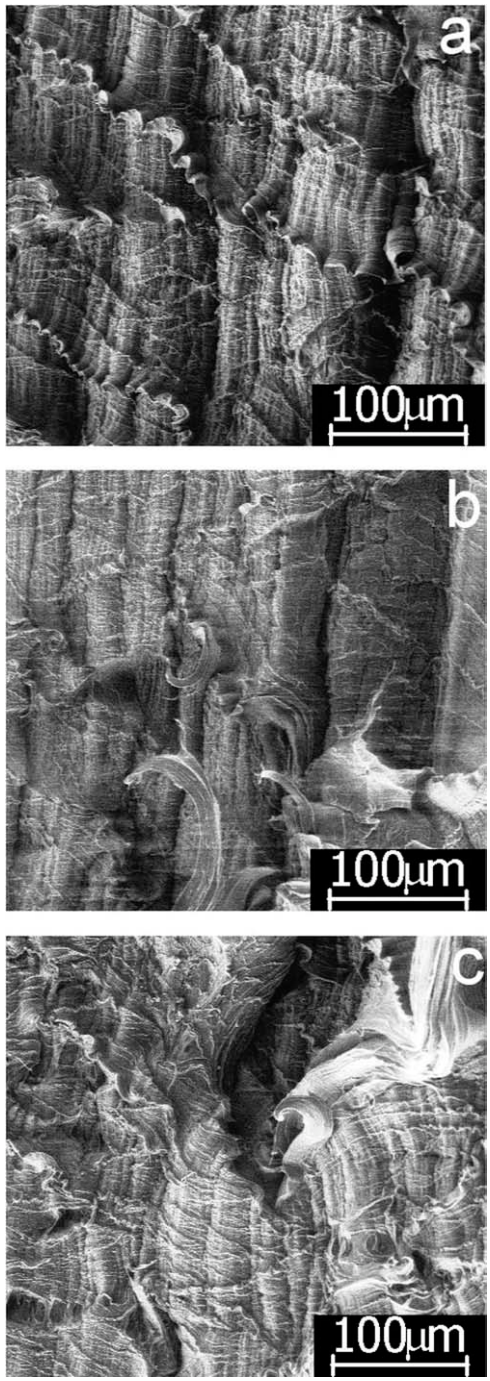

Figure 6 SEM micrographs of fractured surfaces of (a) PE, (b) e-PE, and (c) e-PE/g, focused on the regions of ductile fracture.

increases in this order: PE (204 J/m^2) < e-PE/g (220 J/m^2) < e-PE (242 J/m^2). Micrographs of the fractured areas of the materials are shown in Figure 6. The images were recorded in the regions of ductile fracture. All the materials are characterized by the presence of bands containing fibrils that are evidence of microplasticity. When comparing e-PE [Fig. 6(b)] or e-PE/g [Fig. 6(c)] with PE [Fig. 6(a)], longer fibrils are noted. This indicates that the extruded materials exhibit more plastic deformation before failure than nonextruded material, and supports the macroscopic measurements (Fig. 5). Impact behavior of PE, e-PE, and e-PE/g is in line with their bending behavior (Fig. 7). Indeed, the dissipated energy during the impact, or impact toughness, increases in this order: PE ≈ e-PE/g < e-PE. The high toughness of e-PE can be explained by the presence of randomly oriented textured meso-domains that enhance plasticity and limit damage. Indeed, it is thought that crack propagation is hindered in e-PE by the presence of textured meso-domains whose chain orientation is perpendicular to the crack propagation direction. In this case, a high stress transfer will occur from amorphous layers to crystalline lamellae that will deform plastically via chain slip mechanisms to withstand the stresses generated by the crack propagation. These mechanisms are also active in the composite e-PE/g, but the presence of graphite has the opposite effect in term of toughness. As shown by SEM investigation [Fig. 2(c)], a segregation of the graphite on grain boundaries is noted, leading to consolidation defects. Such defects may induce intergranular separation processes, and hence, damage mechanisms instead of plastic mechanisms to dissipate the stress induced by the crack propagation. This obviously reduces the toughness of the material. The granular microstructure of PE, e-PE, and e-PE/g is represented in Figure 8. The reference material (PE) [Fig. 8(a)] contains polymer grains with a quite random chain orientation as demonstrated by WAXS [Fig. 1(b)]. Regarding e-PE [Fig. 8(b)], the combination of microextrusion and compression-molding leads to an orientation of polymer chain as shown by WAXS [Fig. 1(c,d)]. We also hypothesize that some areas of e-PE are highly consolidated. This could be the case inside the extruded pellets, but further investigations are required to

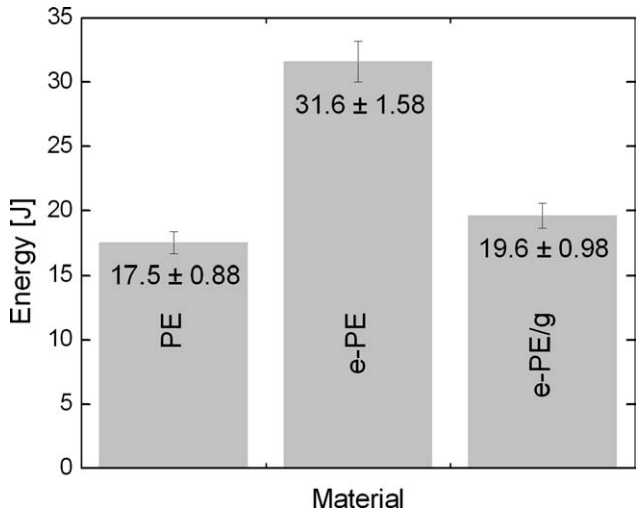

Figure 7 Impact behavior of PE, e-PE, and e-PE/g.

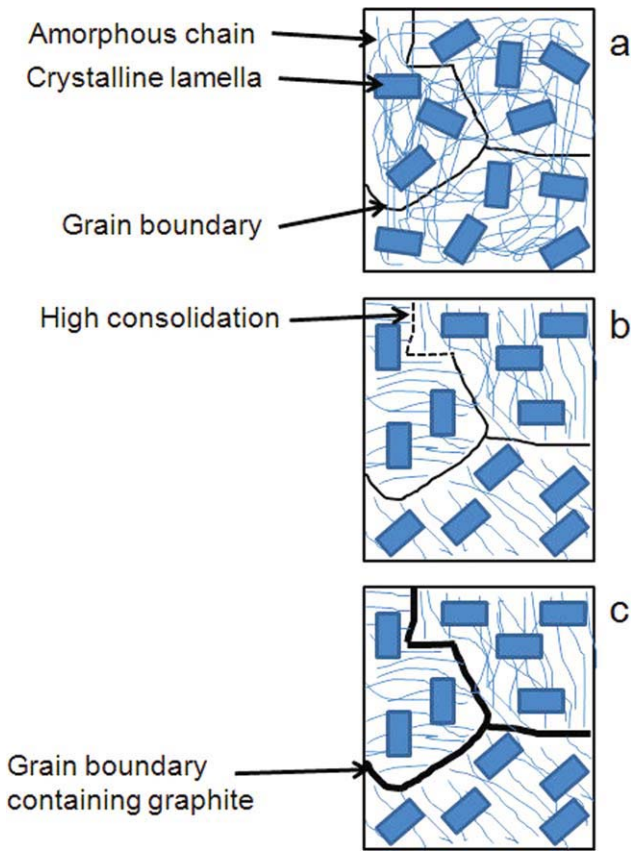

Figure 8 Schematic representation of (a) PE, (b) e-PE, and (c) e-PE/g. [Color figure can be viewed in the online issue, which is available at wileyonlinelibrary.com.].

verify this point. The composite UHMWPE/graphite (e-PE/g) [Fig. 8(c)] exhibits the same textured granular microstructure than neat extruded UHMWPE (e-PE), but in this case the presence of graphite at the surface of the grains generates a low consolidation during the processing.

Surface mechanical behavior

Scratch grooves of the investigated materials are shown in Figure 9, while the scratch characteristics are reported in Table I. The materials exhibit a similar scratch behavior characterized by a viscoelastoplastic mode with any damage.[19] It is to be noted that the thin parallel scratches present in the groove of PE [Fig. 9(a)] and e-PE/g [Fig. 9(c)] were not damage phenomena generated by the scratching procedure, but were defects initially present at the surface of the material. The neat extruded material, e-PE, has the lowest friction coefficient μ equal to 0.77, while the two other materials, PE and e-PE/g, have a friction coefficient equal to 0.83. The penetration depth of the extruded materials, e-PE and e-PE/g, is lower than that of the reference material (41–42 μm vs. 44 μm). The surface recovery is similar for the three materials (r of about 65%). As stipulated in the article of Addiego et al.,[16] the lower the coefficient of friction, the lower the work done during the viscoelastoplastic deformation generated by scratching. Consequently, e-PE is characterized by a low scratching work that may be due to a higher

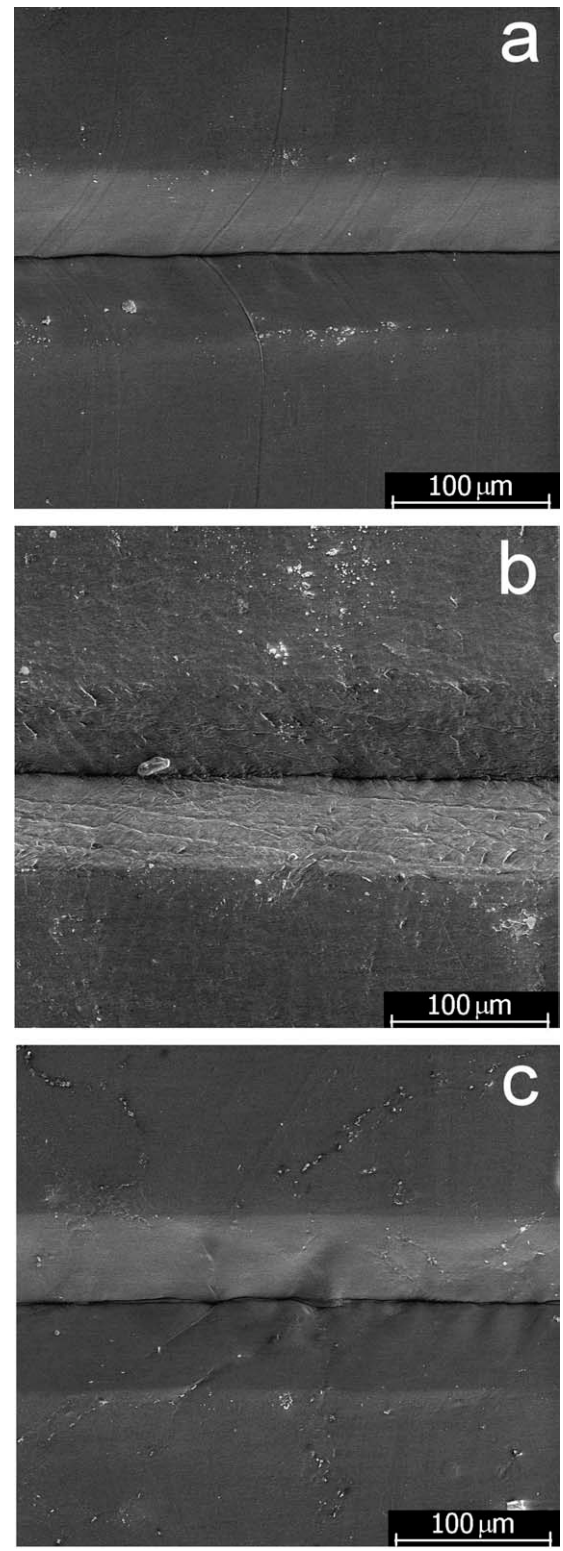

Figure 9 SEM micrographs of scratch grooves generated on (a) PE, (b) e-PE, and (c) e-PE/g.

TABLE I
Scratch Tests Characteristics of PE, e-PE, and e-PE/g

Scratch characteristic	PE	e-PE	e-PE/g
Friction coefficient μ (mN/mN)	0.83 ± 0.01	0.77 ± 0.01	0.83 ± 0.01
Penetration depth P_d (μm)	44.11 ± 0.56	41.72 ± 0.77	40.74 ± 0.63
Residual depth R_d (μm)	14.96 ± 1.21	15.38 ± 1.41	13.93 ± 1.17
Surface recovery r (%)	66.08 ± 3.17	63.13 ± 3.57	65.80 ± 3.40

consolidation when compared to PE and e-PE/g, as shown by SEM (Fig. 2). Indeed, crossing a lower number of structural defects may reduce the scratching work. We hence concluded that neat extruded UHMWPE has anti-friction properties. The lower penetration depth of the extruded materials (e-PE and e-PE/g) may be linked to the presence of textured grains in these materials that locally increase the strength and hence limit the tip penetration. It was expected that the higher the local strength, the higher the surface recovery would be. Nevertheless, this is not the case since the three materials exhibit a similar surface recovery despite their different values of penetration depth (Table I). It is thought that the recovery of the materials was not totally achieved when the residual groove depth was measured. Note that R_d was measured just after the end of the scratching, but in the case of polymers it is well-known that the viscoelastic relaxation may take several hours.[20]

The sliding wear behavior of PE, e-PE, and e-PE/g is displayed in Figure 10. Whatever the material, the dissipated energy increases with the number of cycles and stabilizes from about 40,000 cycles [Fig. 10(a)]. The initial increase of dissipated energy is considered as the running-in wear phenomenon and, after this stage, the steady-state of sliding wear is achieved. The neat materials PE and e-PE have shown similar sliding behavior. The presence of graphite within UHMWPE significantly disturbs the running-in sliding process as indicated by the presence of small bumps on the curve dissipated energy-number of cycles. During wear sliding experiments, the running-in process is linked to the smoothing of rough areas, and to the overcoming of physical interactions between the counterface and the tested material. The running-in process is similar for the neat materials; since, the chemical composition is the same (same physical interactions with the counterface) and the same mold was used to process the plates (same roughness). Regarding the composite e-PE/g, we also used the same mold but the presence of graphite may perturb the physical interactions between the counterface and the polymer matrix, which may explain the presence of bumps on the sliding dissipated energy curve. These bumps can also be because of delamination mechanisms of the graphite platelets, but further investigations are required to check the occurrence of this mechanism. Regarding the cumulative dissipated energy [Fig. 10(b)], one notes a linear increase of this energy with the number of cycles. At 50,000 cycles, ΣE_d increases in this order: e-PE (92,000 μJ) ≈ PE (100,000 μJ) < e-PE/g (112,000 μJ). It is to be noted that the low number of cycles performed in this study does not enable to calculate a wear loss volume with enough precision. As first approximation, we consider that the lower the cumulative energy, the lower the wear volume. Indeed, it is generally accepted that wear volume increases linearly with the dissipated energy.[13,21] Thus, when compared to the reference UHMWPE, neat extruded UHMWPE may have a similar wear resistance, while extruded UHMWPE with graphite may have a decreased wear resistance.

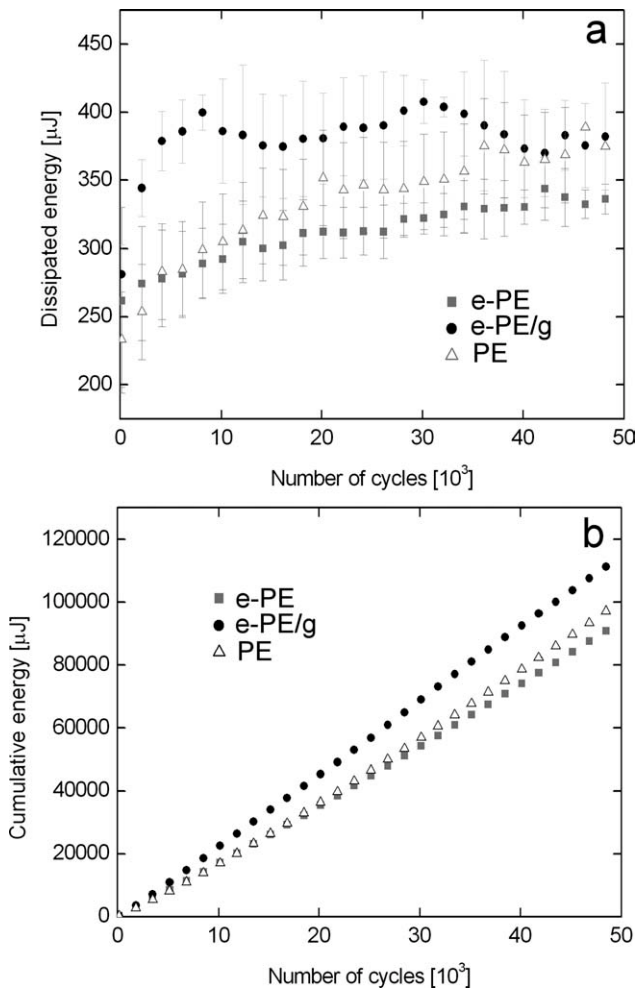

Figure 10 Sliding wear behavior of PE, e-PE, and e-PE/g, (a) evolution of dissipated energy as a function of cycles number and (b) evolution of cumulative dissipated energy as a function of cycles number.

CONCLUSIONS

A new processing route combining swelling in toluene, microextrusion, and compression-molding to produce UHMWPE/graphite nanoplatelets composites was developed in this article. This methodology leads to a nanocomposite having a poor filler distribution and a nonoptimal consolidation in comparison with the reference compression-molded UHWMPE. The mechanical properties of the nanocomposite are unsatisfactory in terms of tensile behavior (brittle behavior) and wear sliding behavior (high dissipated energy), which confirms the inefficiency of compounding UHMWPE with fillers. We however found that the bending and impact toughness of UHMWPE composites is satisfactory. It is suggested that UHMWPE/graphite nanoplatelets composites could be suitable in application where a conductive polymer is required. Indeed, due to the localization of graphite at the grains surface, we expect the presence of a continuous conductive path. When the here proposed processing route was applied to neat UHWMPE, a higher tensile strength, a higher bending and impact toughness, and a lower coefficient of friction were obtained as compared to the reference UHMWPE. We also found that the wear behavior of neat microextruded UHMWPE is similar to that of the reference material. These first results demonstrate that the durability of UHMWPE that is often dictated by bulk and surface mechanical properties, as for medical or machine construction applications, could be increased by our new processing route. However, to verify the generality of our results, further investigations are required. To this end, bulk and surface mechanical properties of neat microextruded UHWMPE are currently evaluated in a wider range of experimental conditions (temperature, rate, frequency, number of cycles, etc. . .).

The authors wish to acknowledge Pr. Jean-Pierre Celis (KU Leuven, Belgium) for the wear sliding tests, and Ticona Benelux (Bruxelles, Belgium) for providing UHMWPE powder.

References

1. Han, K. S.; Wallace, J. F.; Truss, R. W.; Geil, P. H. J Macromol Sci Phys 1981, B19, 313.
2. Wang, X. Y.; Li, S. Y.; Salovey, R. J Appl Poly Sci 1988, 35, 2165.
3. Barbeston, A.; Hornsby, P. R. J Mater Sci Lett 1995, 14, 80.
4. Kurtz, S. M. In UHMWPE Biomaterials Handbook; Kurtz, S. M., Ed.; Academic Press: Burlington, MA, 2009; Chapter 2.
5. Fang, L.; Leng, Y.; Gao, P. Biomaterials 2005, 26, 3471.
6. Sclippa, E.; Pierarski, K. J Biomed Mater Res 1973, 7, 59.
7. Wood, W. J.; Maguire, R. G.; Zhong, W. H.; Compos B 2011, 42, 584.
8. Martinez-Morlanes, M. J.; Castell, P.; Martinez, V.; Benito, A.; Maser, W.; Martinez, M. T.; Puertolas, J. A. Fourth International Meeting UHMWPE for Arthroplasty: from powder to debris, September 16th–17th, 2009, Torino, Italy.
9. Tong, J.; Ma, Y.; Jiang, M. Wear 2003, 255, 734.
10. Zoo, Y. S.; An, J. W.; Lim, D. P.; Lim, D. S. Tribol Lett 2004, 16, 305.
11. Tetik, R. D.; Galante, J. O.; Rostoker, W. J Biomed Mater Res 1974, 8, 231.
12. Pruitt, L.; Bailey, L. Polymer 1998, 39, 1545.
13. Mohrbacher, H.; Celis, J. P.; Roos, J. R. Tribol Int 1995, 28, 269.
14. Addiego, F.; Di Martino, J.; Ruch, D.; Dahoun, A.; Godard, O.; Lipnik, P.; Biebuyck, J. J. Polym Eng Sci 2010, 50, 278.
15. Bakshi, S. R.; Tercero, J. E.; Agarwal, A. Compos A 2007, 38, 2493.
16. Addiego, F.; Buchheit, O.; Ruch, D.; Ahzi, S.; Dahoun, A. Clin Orthop Relat Res 2011, 469, 2318.
17. Boontongkong, Y.; Cohen, R. E.; Spector, M.; Bellare, A. Polymer 1998, 39, 6391.
18. Galeski, A. Prog Polym Sci 2003, 28, 1643.
19. Briscoe, B. J.; Pelillo, E.; Sinha, S. K.; Evans, P. D. Wear 1996, 200, 137.
20. Addiego, F.; Dahoun, A.; G'Sell, C.; Hiver, J. M. Polymer 2006, 47, 4387.
21. Berradja, A.; Willems, G.; Celis, J. P. Aust Orthodontic J 2006, 22, 21.